AMERICAN SOCIETY FOR MICROBIOLOGY | Journal of Bacteriology®

RESEARCH ARTICLE

FliK-Driven Conformational Rearrangements of FlhA and FlhB Are Required for Export Switching of the Flagellar Protein Export Apparatus

Tohru Minamino,[a] Yumi Inoue,[a]* Miki Kinoshita,[a] Keiichi Namba[a,b,c]

[a]Graduate School of Frontier Biosciences, Osaka University, Suita, Osaka, Japan
[b]RIKEN Spring-8 Center and Center for Biosystems Dynamics Research, Suita, Osaka, Japan
[c]JEOL Yokogushi Research Alliance Laboratories, Osaka University, Suita, Osaka, Japan

ABSTRACT FlhA and FlhB are transmembrane proteins of the flagellar type III protein export apparatus, and their C-terminal cytoplasmic domains ($FlhA_C$ and $FlhB_C$) coordinate flagellar protein export with assembly. $FlhB_C$ undergoes autocleavage between Asn-269 and Pro-270 in a well-conserved NPTH loop located between $FlhB_{CN}$ and $FlhB_{CC}$ polypeptides and interacts with the C-terminal domain of the FliK ruler when the length of the hook has reached about 55 nm in *Salmonella*. As a result, the flagellar protein export apparatus switches its substrate specificity, thereby terminating hook assembly and initiating filament assembly. The mechanism of export switching remains unclear. Here, we report the role of $FlhB_C$ cleavage in the switching mechanism. Photo-cross-linking experiments revealed that the *flhB*(*N269A*) and *flhB*(*P270A*) mutations did not affect the binding affinity of $FlhB_C$ for FliK. Genetic analysis of the *flhB*(*P270A*) mutant revealed that the P270A mutation affects a FliK-dependent conformational change of $FlhB_C$, thereby inhibiting the substrate specificity switching. The *flhA*(*A489E*) mutation in $FlhA_C$ suppressed the *flhB*(*P270A*) mutation, suggesting that an interaction between $FlhB_C$ and $FlhA_C$ is critical for the export switching. We propose that the interaction between $FliK_C$ and a cleaved form of $FlhB_C$ promotes a conformational change in $FlhB_C$ responsible for the termination of hook-type protein export and a structural remodeling of the $FlhA_C$ ring responsible for the initiation of filament-type protein export.

IMPORTANCE The flagellar type III protein export apparatus coordinates protein export with assembly, which allows the flagellum to be efficiently built at the cell surface. Hook completion is an important morphological checkpoint for the sequential flagellar assembly process. The protein export apparatus switches its substrate specificity from the hook protein to the filament protein upon hook completion. FliK, FlhB, and FlhA are involved in the export-switching process, but the mechanism remains a mystery. By analyzing a slow-cleaving *flhB*(*P270A*) mutant, we provide evidence that an interaction between FliK and FlhB induces conformational rearrangements in FlhB, followed by a structural remodeling of the FlhA ring structure that terminates hook assembly and initiates filament formation.

KEYWORDS bacterial flagella, FlhA, FlhB, FliK, hook length control, substrate specificity switching, type III protein secretion

The bacterial flagellum is responsible for swimming motility in liquid media and for swarming motility on solid surfaces for many bacterial species. The flagellum is composed of a basal body (rotary motor), a hook (universal joint), and a filament (helical propeller). Flagellar assembly begins with the basal body, followed by the hook and finally the filament (1). For assembly of the hook and filament from the cell surface, a

Citation Minamino T, Inoue Y, Kinoshita M, Namba K. 2020. FliK-driven conformational rearrangements of FlhA and FlhB are required for export switching of the flagellar protein export apparatus. J Bacteriol 202:e00637-19. https://doi.org/10.1128/JB.00637-19.

Editor Ann M. Stock, Rutgers University-Robert Wood Johnson Medical School

Address correspondence to Tohru Minamino, tohru@fbs.osaka-u.ac.jp.

* Present address: Yumi Inoue, Department of Ophthalmology and Visual Sciences, Kyoto University Graduate School of Medicine, Kyoto, Japan.

Received 7 October 2019
Accepted 6 November 2019
Accepted manuscript posted online 11 November 2019
Published 15 January 2020

type III protein export apparatus transports these component proteins from the cytoplasm to the distal end of the growing structure. The type III protein export apparatus is composed of five transmembrane proteins, FlhA, FlhB, FliP, FliQ, and FliR and three cytoplasmic proteins, FliH, FliI, and FliJ (2).

The length of the hook is controlled, extending about 55 nm from the cell surface in wild-type cells of *Salmonella enterica* serovar Typhimurium (here referred to *Salmonella*) (3). The flagellar type III protein export apparatus uses the FliK ruler to measure the hook length and facilitates the switching of export specificity from hook-type substrates (FlgD, FlgE, and FliK) to filament-type ones (FlgK, FlgL, FlgM, FliC, and FliD) upon hook completion. The substrate specificity switch terminates hook assembly and initiates filament assembly. FlhB and FlhA are directly involved in export switching of the type III protein export apparatus (4).

FliK consists of N-terminal ($FliK_N$) and C-terminal ($FliK_C$) domains (5, 6). $FliK_N$ acts as a molecular ruler to measure the length of the hook through interactions of $FliK_N$ with the hook-capping protein FlgD and the hook protein FlgE (7–11), whereas $FliK_C$ interacts with the C-terminal cytoplasmic domain of FlhB ($FlhB_C$) to promote substrate specificity switching of the flagellar type III protein export apparatus (12–15).

$FlhB_C$ consists of $FlhB_{CN}$ and $FlhB_{CC}$ polypeptides with molecular weights of 8.5 and 11.5 kDa, respectively (16, 17). A conserved hydrophobic patch formed by Ala-286, Pro-287, Ala-341, and Leu-344 residues in $FlhB_{CC}$ is involved in the interaction of $FlhB_C$ with the N-terminal segments of FlgD, FlgE, and FliK, which contain an export signal recognized by the flagellar type III protein export apparatus (18). Autocatalytic cleavage between Asn-269 and Pro-270, which is located within a highly conserved NPTH loop between $FlhB_{CN}$ and $FlhB_{CC}$, is critical for export switching of the protein export apparatus (19, 20). It has been reported that autocleavage of the C-terminal cytoplasmic domain of SpaS, which is a FlhB homologue of the *Salmonella* SPI-1 injectisome, allows the proper conformation of $SpaS_C$ to render it competent for its switching function (21), but it remains unclear how its cleaved form flips export specificity of the type III protein export apparatus of the *Salmonella* SPI-1 injectisome.

FlhA forms a homo-nonamer through its C-terminal cytoplasmic domain ($FlhA_C$) in the flagellar type III protein export apparatus (22). $FlhA_C$ interacts with flagellar chaperones in complex with their cognate filament-type substrates to promote the export of filament-type proteins to form the flagellar filament at the hook tip (23–26). Interactions of a flexible linker of FlhA ($FlhA_L$) with its neighboring $FlhA_C$ subunit in the ring structure induce the remodeling of the $FlhA_C$ ring structure upon completion of the hook structure, thereby allowing the flagellar chaperones in complex with their cognate substrates to bind to the $FlhA_C$ ring to facilitate the export of filament-type proteins (27, 28). However, it remains unknown which protein triggers the structural remodeling of the $FlhA_C$ ring structure.

The *flhB*(*N269A*) mutation inhibits not only autocleavage of $FlhB_C$ but also substrate specificity switching of the flagellar type III protein export apparatus (19), leading to a plausible hypothesis that an interaction between $FliK_C$ and a cleaved form of $FlhB_C$ may induce the structural remodeling of the $FlhA_C$ ring responsible for the substrate specificity switching. To clarify this hypothesis, we analyzed a slow-cleaving *flhB*(*P270A*) mutant in detail and provide evidence suggesting that the binding of $FliK_C$ to a cleaved form of $FlhB_C$ not only terminates hook polymerization but also induces conformational rearrangements of the $FlhA_C$ ring to initiate filament assembly at the hook tip.

RESULTS

Effect of the *flhB*(*N269A*) and *flhB*(*P270A*) mutations on photo-cross-linking between $FliK_C$ and $FlhB_C$. A well-conserved Ile-304 residue of FliK is critical for substrate specificity switching of the flagellar type III protein export apparatus (14). Recently, it has been shown that Ile-304 of $FliK_C$ is in relatively close proximity to $FlhB_C$, allowing FliK to form a photo-cross-linked product with $FlhB_{CC}$ (15). To investigate whether autocleavage of $FlhB_C$ is required for the interaction of $FlhB_C$ with $FliK_C$, photo-cross-linking experiments were conducted using a photoreactive phenylalanine, *p*-benzoyl-phenylalanine (pBPA), that

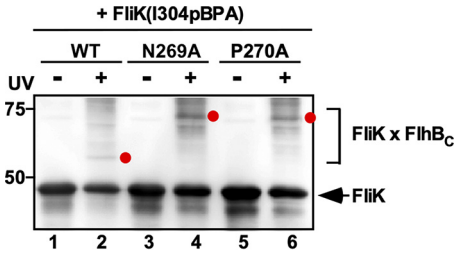

FIG 1 Effect of the *flhB*(*N269A*) and *flhB*(*P270A*) mutations on photo-cross-linking between FliK$_C$ and FlhB$_C$. *E. coli* BL21 Star(DE3) cells coexpressing FliK(I304pBPA) with FlhB$_C$, FlhB$_C$(N269A), or FlhB$_C$(P270A) were UV irradiated for 5 min (+) or not irradiated (–) and then analyzed by immunoblotting with polyclonal anti-FliK antibody. Photo-cross-linked FliK-FlhB$_C$ products are indicated by red dots. The position of free FliK is indicated by an arrow. Molecular mass markers (in kilodaltons) are shown on the left.

was introduced into an amber codon at position 304 of FliK using the amber suppressor tyrosyl tRNA and the engineered tyrosyl-tRNA synthetase (29). In agreement with a previous report (15), UV irradiation of FliK(I304pBPA) reproducibly produced a ca. 53-kDa photo-cross-linked product with FlhB$_{CC}$ when coexpressing with wild-type FlhB$_C$ (Fig. 1, lane 2). Photo-cross-linked products were also seen when FliK(I304pBPA) was coexpressed with FlhB$_C$(N269A) and FlhB$_C$(P270A) (Fig. 1, lanes 4 and 6). In contrast to wild-type FlhB$_C$, which is cleaved into FlhB$_{CN}$ and FlhB$_{CC}$ polypeptides in an autocatalytic manner, FlhB$_C$(N269A) and FlhB$_C$(P270A) do not undergo autocleavage. As a result, the molecular mass of the FliK-FlhB$_C$ heterodimer is estimated to be ca. 64 kDa, which is the sum of the molecular masses of FliK (42 kDa) and noncleaved FlhB$_C$ (22 kDa), respectively. This mass is almost the same as that of the cross-linked products detected on immunoblots. Therefore, we suggest that the *flhB*(*N269A*) and *flhB*(*P270A*) mutations do not interfere with the interaction of FlhB$_C$ with FliK.

Effect of the *flhB*(*N269A*) and *flhB*(*P270A*) mutations on hook length. The *flhB*(*N269A*) and *flhB*(*P270A*) mutants produce polyhooks (10, 19). We found that the *flhB*(*N269A*) and *flhB*(*P270A*) mutations do not affect the interaction of FlhB$_C$ with FliK, raising the question of whether the FliK-FlhB$_C$ interaction influences the rate of hook assembly. To clarify this question, we purified polyhook-basal bodies from these two *flhB* mutants and measured the length of each polyhook. The average hook lengths of the *flhB*(*N269A*) and *flhB*(*P270A*) mutants were 127.4 ± 85.6 nm ($n = 237$) and 125.6 ± 77.9 nm ($n = 251$), respectively, which were much longer than the wild-type length with a wide size distribution (53.5 ± 7.5 nm, $n = 103$) but shorter than the length of the polyhook produced by the *fliK* null mutant (418.5 ± 228.5 nm, $n = 332$) (Fig. 2). When a Δ*fliK*::*tetRA* allele was introduced into the *flhB*(*N269A*) and *flhB*(*P270A*) mutants by P22-mediated transduction, the average lengths of the polyhooks produced by the *flhB*(*N269A*) Δ*fliK*::*tetRA* and *flhB*(*P270A*) Δ*fliK*::*tetRA* mutants were 331 ± 198.9 nm ($n = 316$) and 319.1 ± 169.9 nm ($n = 318$) (Fig. 2). These results suggest that the FliK-FlhBc interaction reduces the hook polymerization rate significantly.

Isolation of pseudorevertants form the *flhB*(*P270A*) mutant. To clarify the role of autocleavage of FlhB$_C$ on substrate specificity switching of the flagellar type III protein export apparatus, we isolated five pseudorevertants from the *flhB*(*P270A*) mutant. The motility of these pseudorevertants was better than that of their *flhB*(*P270A*) mutant, although it was not as good as that of the wild-type strain (Fig. 3A). P22-mediated genetic mapping showed that the gain-of-function mutations were located within the *flhBAE* operon. DNA sequencing identified two missense mutations, T268I (isolated two times) and E314A (isolated two times) in FlhB$_C$, and a missense mutation, A489E, in FlhA$_C$ (Fig. 3B).

To test whether these suppressor mutations shorten the length of the polyhooks produced by the *flhB*(*P270A*) mutant, we isolated flagella from the *flhB*(*P270A/E314A*) and *flhB*(*P270A*) *flhA*(*A489E*) suppressor mutants and measured the hook length. The hook lengths of the *flhB*(*P270A/E314A*) and *flhB*(*P270A*) *flhA*(*A489E*) suppressor mutants

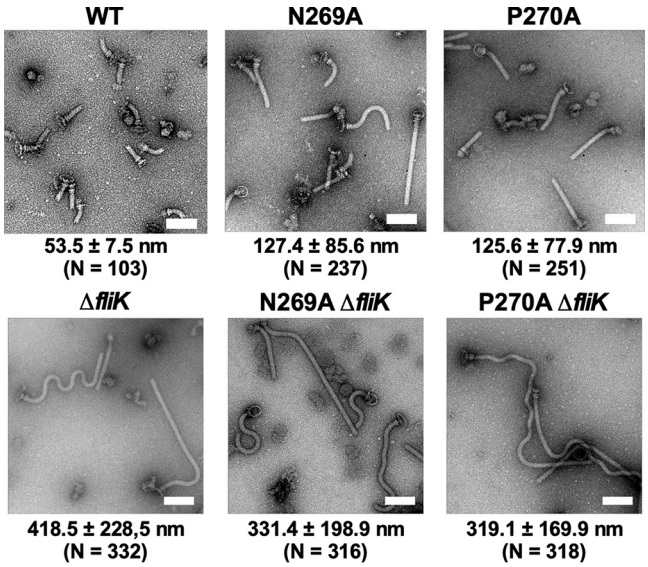

FIG 2 Effect of *flhB*(*N269A*) and *flhB*(*P270A*) mutations on hook length control. Electron micrograms of hook-basal bodies isolated from SJW1103 (wild type, indicated as WT), TH13763 [*flhB*(*N269A*), indicated as N269A], TH12499 [*flhB*(*P270A*), indicated as P270A], MM1103iK (Δ*fliK*), TH13763iK (N269A Δ*fliK*), and TH12499iK (P270A Δ*fliK*) are shown. The average hook length and standard deviations are shown. *N*, number of hook-basal bodies and polyhook-basal bodies, which were measured. Scale bars, 100 nm.

were 97.7 ± 65.5 nm ($n = 129$) and 102.6 ± 62.8 nm ($n = 138$) (Fig. 3C) compared to 53.5 ± 7.5 nm ($n = 103$) for wild-type cells and 125.6 ± 77.9 nm ($n = 251$) for the *flhB*(*P270A*) cells (Fig. 2). This indicates that these two suppressor mutations slightly shorten the polyhook length. This suggests that these suppressor mutants still cannot properly terminate the export of FlgE. Consistently, there was no significant difference in the secretion levels of hook-type proteins such as FlgE and FlgD between the *flhB*(*P270A*) mutant and the suppressor mutants (Fig. 3D, first and second rows).

To investigate the export-switching efficiency of the *flhB*(*P270A/T268I*), *flhB*(*P270A/E314A*), and *flhB*(*P270A*) *flhA*(*A489E*) suppressor mutants, we analyzed the secretion levels of FlgK and FliC by immunoblotting with polyclonal anti-FlgK and anti-FliC antibodies, respectively. The levels of FlgK and FliC secreted by these suppressor mutants were higher than those seen in their parent *flhB*(*P270A*) mutant and were almost the same as the wild-type levels (Fig. 3D, third and fourth rows). These results suggest that the *flhB*(*T268I*), *flhB*(*E314A*), and *flhA*(*A489E*) suppressor mutations allow the *flhB*(*P270A*) mutant to initiate the assembly of the filament efficiently.

We tested whether intragenic *flhB*(*T268I*) and *flhB*(*E314A*) suppressor mutations promote autocleavage of $FlhB_C$(P270A). Only the intact form of $FlhB_C$ was detected in whole-cell lysates prepared from *E. coli* BL21 Star(DE3) cells overexpressing His-$FlhB_C$(P270A) (Fig. 3E). In contrast, significant amounts of cleaved forms of $FlhB_C$ were detected in BL21 Star(DE3) cells overexpressing His-$FlhB_C$(P270A/T268I) or His-$FlhB_C$(P270A/E314A) in a way similar to wild-type $FlhB_C$ although their intact forms were also seen (Fig. 3E). These results indicate that the intragenic *flhB*(*T268I*) and *flhB*(*E314A*) suppressor mutations induce a conformational change of the NPTH loop, allowing $FlhB_C$ to undergo autocatalytic cleavage into two distinct $FlhB_{CN}$ and $FlhB_{CC}$ polypeptides. Therefore, we conclude that the autocleavage of $FlhB_C$ is required not only for efficient termination of hook-type protein export but also for the efficient export of filament-type proteins.

Effect of second-site *flhB* and *flhA* mutations on motility. To test whether second-site *flhB* and *flhA* mutations by themselves affect the export-switching function of the flagellar type III protein export apparatus, we introduced these second-site mutations into wild-type FlhB and FlhA by site-directed mutagenesis and analyzed their motility. The motilities of the *flhB*(*T268A*), *flhB*(*E314A*), and *flhA*(*E314A*) mutants were

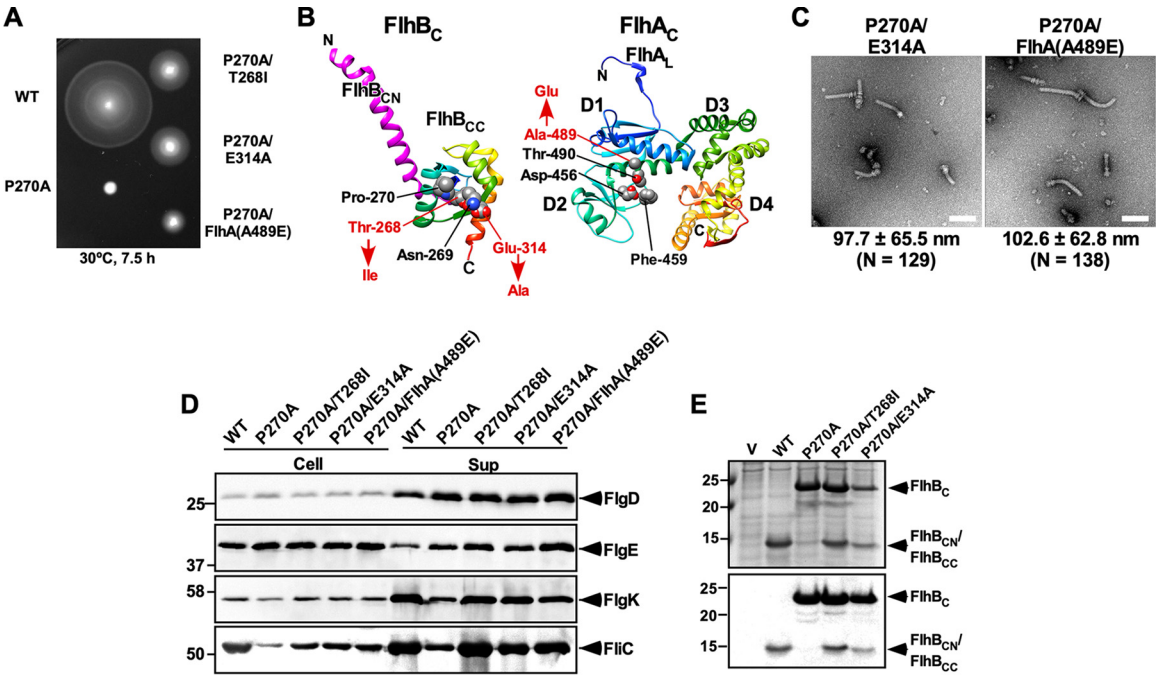

FIG 3 Isolation of pseudorevertants from the *flhB*(*P270A*) mutant. (A) Motilities of SJW1103 (WT), TH12499 (P270A), MMB12499-SP1 [*flhB*(*P270A/T268I*), indicated as P270A/T268I], MMB12499-SP2 [*flhB*(*P270A/E314A*), indicated as P270A/E314A], and MMB12499-SP3 [*flhB*(*P270A*) *flhA*(*A489E*), indicated as P270A/FlhA(A489E)] in soft agar. Plates were incubated at 30°C for 7.5 h. (B) Location of intragenic *flhB*(*T268I*) and *flhB*(*E314A*) suppressor mutations in the crystal structure of FlhB$_C$ (PDB ID 3B0Z) and an extragenic *flhA*(*A489E*) suppressor mutation in the crystal structure of FlhA$_C$ (PDB ID 3A5I). FlhB$_C$ undergoes autocatalytic cleavage between Asn-269 and Pro-270 residues and so is composed of two distinct FlhB$_{CN}$ (magenta) and FlhB$_{CC}$ (rainbow) polypeptides. Well-conserved Asp-456, Phe-459, and Thr-490 residues of FlhA form part of the flagellar chaperone-binding site. The C-α backbone is color-coded from blue to red, going through the rainbow colors from the N terminus to the C terminus. (C) Electron micrograms of hook-basal bodies and polyhook-basal bodies isolated from the MMB12499-SP2 and MMB12499-SP3 strains. The average hook lengths and standard deviations are shown. Scale bars, 100 nm. (D) Secretion assays of FlgD, FlgE, FlgK, and FliC. Immunoblotting using polyclonal anti-FlgD (first row), anti-FlgE (second row), anti-FlgK (third row), or anti-FliC (fourth row) antibody of whole-cell proteins (Cell) and culture supernatants (Sup) from the strains described above. Arrowheads indicate positions of FlgD, FlgE, FlgK, and FliC. The positions of molecular mass markers (in kilodaltons) are given on the left. (E) Effect of *flhB*(*T268I*) and *flhB*(*E314A*) suppressor mutations on autocleavage of FlhB$_C$(P270A). Coomassie blue-stained SDS-PAGE gels of whole-cell proteins prepared from *E. coli* BL21 Star(DE3) cells transformed with pET19b (V), pYI124 (N-terminally His-tagged FlhB$_C$, indicated as WT), pYI140 [His-FlhB$_C$(P270A), indicated as P270A], pYI140-SP1 [His-FlhB$_C$(P270A/T268I), indicated as P270A/T268I], or pYI140-SP2 [His-FlhB$_C$(P270A/E314A), indicated as P270A/E314A] are shown. The positions of the intact form and the cleaved His-FlhB$_{CN}$ and FlhB$_{CC}$ polypeptides are indicated by arrowheads.

almost the same as that of wild-type cells (see Fig. S1A and B in the supplemental material), indicating that these second-site mutations display no significant motility phenotype.

Effect of FliK defect on the export-switching function of the flagellar type III protein export apparatus. To test whether the export-switching function of the *flhB*(*P270A/T268I*), *flhB*(*P270A/E314A*), and *flhB*(*P270A*) *flhA*(*A489E*) suppressor mutants is dependent on FliK, we introduced a Δ*fliK*::*tetRA* allele into these three suppressor mutants by P22-mediated transduction and analyzed the secretion levels of FlgE and FliC. A deletion of the *fliK* gene totally inhibited the export of FliC but not that of FlgE (Fig. S2). This indicates that these suppressor mutations do not induce autonomous export switching of the flagellar type III protein export apparatus in the absence of FliK.

Effect of the *flhA*(*A489E*) mutation on the interaction of FlhA$_C$ with flagellar chaperones in complex with their cognate substrates. Asp-456, Phe-459, and Thr-490 of FlhA are directly involved in the interaction of the FlgN, FliS, and FliT chaperones in complex with their cognate export substrates, FlgK and FlgL, FliC, and FliD, respectively (24–26). The *flhA*(*A489E*) mutation is located in the chaperone-binding site of FlhA$_C$ (Fig. 3B), raising the question of whether the *flhA*(*A489E*) suppressor mutation affects the interaction of FlhA$_C$ with the chaperone/filament-type export substrate complexes. To clarify this question, we carried out pulldown assays by glutathione

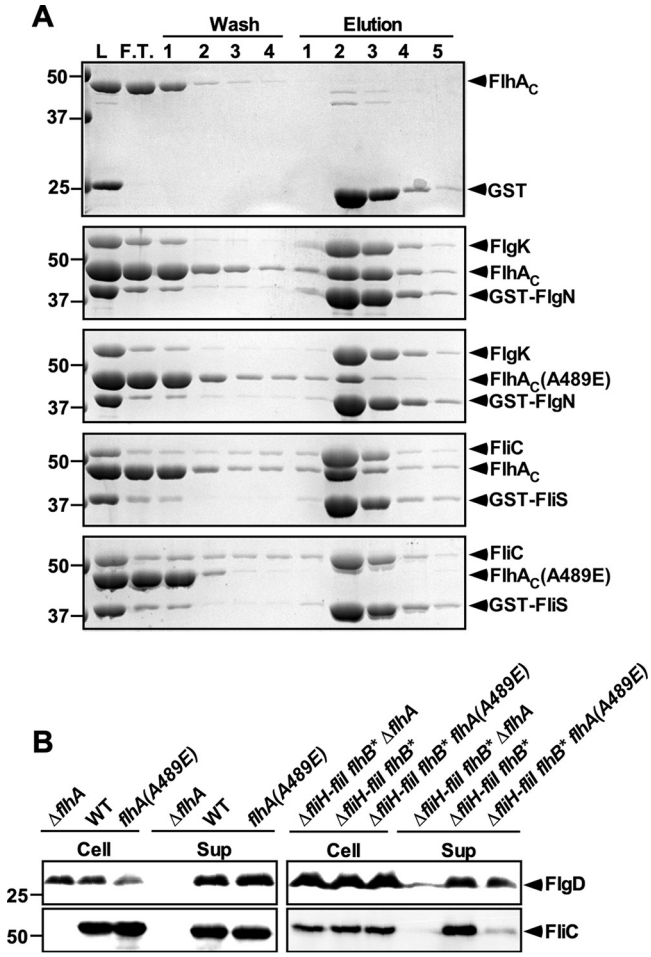

FIG 4 Effect of *flhA*(*A489E*) mutation on the export of filament-type proteins. (A) Effect of the *flhA*(*A489E*) mutation on the interaction of $FlhA_C$ with the FlgN/FlgK and FliS/FliC complexes. Mixtures (L) of purified His-$FlhA_C$ or His-$FlhA_C$(A489E) with GST (first row), GST-FlgN/FlgK (second and third rows), or GST-FliS/FliC (fourth and fifth rows) were purified by GST affinity chromatography. The flowthrough fraction (F.T.), wash fractions, and elution fractions were analyzed by Coomassie brilliant blue staining. Molecular mass markers (in kilodaltons) are given on the left. (B) Secretion assays of FlgD and FliC. Immunoblotting with polyclonal anti-FlgD (first row) or anti-FliC (second row) antibody of whole-cell proteins (Cell) and culture supernatants (Sup) prepared from the *Salmonella* NH001 strain carrying pTrc99AFF4 (indicated as Δ*flhA*), pMM130 (indicated as WT), or pYI130-SP3 [indicated as *flhA*(*A489E*)] and the *Salmonella* NH004 strain (Δ*fliHI flhB** Δ*flhA*) transformed with pTrc99AFF4 (indicated as Δ*fliHI flhB** Δ*flhA*), pMM130 (indicated as Δ*fliHI flhB**), or pYI130-SP3 [indicated as Δ*fliHI flhB* flhA*(*A489E*)] was performed. Arrowheads indicate the positions of FlgD and FliC.

S-transferase (GST) affinity chromatography. $FlhA_C$ coeluted with the GST-FlgN/FlgK and GST-FliS/FliC complexes from a GST column (Fig. 4A, second and fourth rows) but not with GST alone (first row), in agreement with previous reports (24, 25). However, the *flhA*(*A489E*) mutation reduced its binding affinities for the FlgN/FlgK and FliS/FliC complexes (third and fifth rows).

FlhA requires the support of FliH and FliI to fully exert its export function (30–32). When FliH and FliI are missing, much larger amounts of FliC molecules are leaked out into the culture media because the hook-filament junction structure is not formed at the hook tip properly by FlgK and FlgL (32). Although the *flhA*(*A489E*) mutation reduced the binding affinities of $FlhA_C$ for the FlgN/FlgK and FliS/FliC complexes, the *flhA*(*A489E*) mutation increased the secretion levels of FlgK and FliC significantly even in the presence of the *fllhB*(*P270A*) mutation, raising the possibility that FlhA(A489E) requires FliH and FliI to exert its export function. Therefore, we analyzed the effect of the *flhA*(*A489E*) mutation on the filament-type protein export in a Δ*fliH-fliI flhB*(*P28T*)

(Δ*fliH-fliI flhB**) mutant background, of which second-site *flhB*(*P28T*) mutation considerably increases the probability of flagellar formation in the absence of FliH and FliI (33). The motility of the Δ*fliH-fliI flhB*(*P28T*) *flhA*(*A489E*) mutant was worse than that of the Δ*fliH-fliI flhB*(*P28T*) mutant (Fig. S1C). Consistently, the secretion level of FliC was lower in the Δ*fliH-fliI flhB*(*P28T*) *flhA*(*A489E*) mutant than in the Δ*fliH-fliI flhB*(*P28T*) mutant (Fig. 4B, right panel, second row). However, there was no difference in the secretion level of FlgD between these two mutant strains (Fig. 4B, right panel, first row). When FliH and FliI were present, the *flhA*(*A489E*) mutation does not affect the secretion level of FliC at all (Fig. 4C, left panel, second row). These results indicate that FlhA(A489E) requires FliH and FliI to efficiently promote the export of filament-type proteins upon completion of hook assembly. Because the flagellar chaperones in complex with their cognate filament-type substrates bind to the open form of $FlhA_C$ in the $FlhA_C$ ring structure but not to the closed form (26, 28), we propose that the $FlhA_C$(A489E) ring structure may adopt the open form to allow the flagellar type III protein export apparatus to promote the export of filament-type proteins in the presence of the *flhB*(*P270A*) mutation.

Effect of *flhB*(*G293R*), *flhB*(*G293V*), and *flhB*(*A298V*) mutations on export switching. The *flhB*(*G293R*), *flhB*(*G293V*), and *flhB*(*A298V*) mutations in $FlhB_{CC}$ were originally isolated as extragenic *fliK* suppressor mutations to support filament assembly even in the absence of FliK (13). Motility of the *flhB*(*G293R*), *flhB*(*G293V*), and *flhB*(*A298V*) mutants is worse than the wild-type level and much better than that of the *flhB*(*N269A*) and *flhB*(*P270A*) mutants (Fig. 5A). The *flhB*(*G293R*), *flhB*(*G293V*), and *flhB*(*A298V*) mutations significantly affect autocleavage of $FlhB_C$ (16), raising a question about the impact of these *flhB* mutations on the export switching of the flagellar type III protein export apparatus. To clarify this question, we analyzed the levels of filament-type proteins secreted by the *flhB*(*G293R*), *flhB*(*G293V*), and *flhB*(*A298V*) mutants. These three *flhB* mutations reduced the secretion levels of FlgK and FliC by approximately 60% of the wild-type levels (Fig. 5B), confirming that $FlhB_C$ cleavage is required for the efficient export of filament-type proteins.

To investigate whether the *flhB*(*G293R*), *flhB*(*G293V*), and *flhB*(*A298V*) mutations affect hook length control, we prepared hook-basal bodies from these *flhB* mutants and measured their hook length. The average hook lengths of the *flhB*(*G293R*) and *flhB*(*A298V*) mutants were 63.4 $\pm$ 20.2 nm ($n = 107$) and 66.4 $\pm$ 28.1 nm ($n = 128$) (Fig. 5C) compared to (53.5 $\pm$ 7.5 nm, $n = 103$) for the wild-type (Fig. 2), suggesting that the *flhB*(*G293R*) and *flhB*(*A298V*) mutants cannot terminate the export of FlgE at an appropriate timing of hook assembly, thereby causing a loose hook length control. Consistently, the levels of FlgE secreted by the *flhB*(*G293R*) and *flhB*(*A298V*) mutants were about 1.4-fold higher than the wild-type level (Fig. 5B). In contrast, hook length control was not affected by the *flhB*(*G293V*) mutation (Fig. 5C), suggesting that the *flhB*(*G293V*) mutation affects the initiation of filament formation but not the termination of hook assembly.

DISCUSSION

An interaction between $FliK_C$ and $FlhB_C$ triggers substrate specificity switching of the flagellar type III protein export apparatus from the hook protein to the filament protein when the length of the hook has reached about 55 nm in *Salmonella* (4). Autocatalytic cleavage between Asn-269 and Pro-270 within the conserved NPTH loop occurs through a chemical reaction involving cyclization of Asp-269 (20, 34). A conformational change of $FlhB_{CC}$ through a remodeling of hydrophobic interaction networks in $FlhB_{CC}$ is postulated to be responsible for the substrate specificity switching (35). However, little is known about the role of the autocleavage of $FlhB_C$ in the export-switching mechanism. Here, we showed that the *flhB*(*N269A*) and *flhB*(*P270A*) mutations did not affect the interaction of $FlhB_C$ with $FliK_C$ (Fig. 1). We also found that the lengths of polyhooks produced by the *flhB*(*N269A*) and *flhB*(*P270A*) mutants were shorter than that of the *fliK* null mutant (Fig. 2). Introduction of the *fliK* null mutation into these two *flhB* mutants increased the length of the polyhook considerably (Fig. 2). Therefore, we propose that the binding of $FliK_C$ to $FlhB_C$ induces conformational rearrangements of

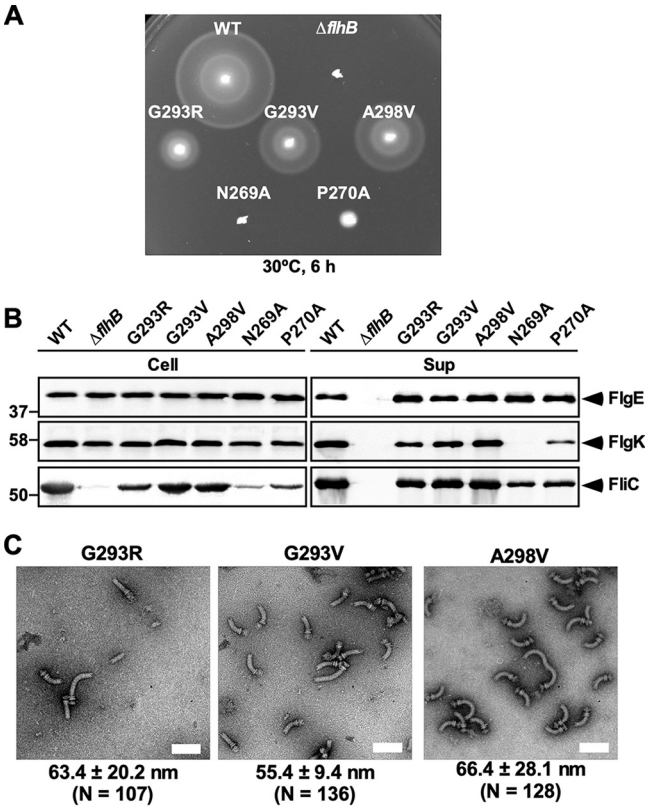

FIG 5 Effect of *flhB*(*G293R*), *flhB*(*G293V*), and *flhB*(*A298V*) mutations on substrate specificity switching of the flagellar type III protein export apparatus. (A) Motility of SJW1103 (WT), MKM50 (Δ*flhB*), MMB2714 [*flhB*(*G293R*), indicated as G293R], MMB3201 [*flhB*(*G293V*), indicated as G293V], MMB2701 [*flhB*(*A298V*), indicated as A298V], TH13763 [*flhB*(*N269A*), indicated as N269A], and TH12499 [*flhB*(*P270A*), indicated as P270A] in soft agar. Plates were incubated at 30°C for 6 h. (B) Secretion assays of FlgE, FlgK, and FliC. Immunoblotting with polyclonal anti-FlgE (first row), anti-FlgK (second row), or anti-FliC (third row) antibody of whole-cell proteins (Cell) and culture supernatants (Sup) prepared from the above strains was performed. Arrowheads indicate the positions of FlgE, FlgK, and FliC. Molecular mass markers (in kilodaltons) are given on the left. (C) Electron micrograms of hook-basal bodies and polyhook-basal bodies isolated from the MMB2714, MMB3201, and MMB2701 strains. The average hook length and standard deviations are shown. Scale bars, 100 nm.

$FlhB_{CC}$ to terminate the export of hook-type proteins and that the autocleavage of $FlhB_C$ is required for proper conformational changes of $FlhB_C$ in a FliK-dependent manner.

The C-terminal cytoplasmic domain EscU ($EscU_C$), which is a FlhB homologue of the injectisome of pathogenic *E. coli*, undergoes autocleavage into $EscU_{CN}$ and $EscU_{CC}$ in a way similar to $FlhB_C$ (34). Structural comparison between $EscU_C$ and $EscU_C$(P263A) has revealed that the *escU*(*P263A*) mutation does not induce a large conformational change of the entire $EscU_C$ structure (Fig. S3A) (34). However, Ala-263 makes hydrophobic contacts with Lys-261, Asn-262, and Glu-307, whereas Pro-263 does not (see Fig. S3A in the supplemental material), suggesting that the conformational flexibility of the conserved NPTH loop connecting between $EscU_{CN}$ and $EscU_{CC}$ could be restricted by a replacement of Pro-270 by Ala, thereby suppressing the autocleavage of $EscU_C$. Here, we found that the intragenic *flhB*(*T268I*) and *flhB*(*E314A*) suppressor mutations facilitated the autocleavage of $FlhB_C$(P270A) to a significant degree (Fig. 3E). Thr-268 and Glu-314 of $FlhB_C$ correspond to Lys-261 and Glu-307 of $EscU_C$, suggesting that the *flhB*(*T268I*) and *flhB*(*E314A*) suppressor mutations affect hydrophobic interactions of Ala-270 with Thr-268, Asn-269, and Glu-307 to allow Asn-269 to be exposed to solvent to induce the autocleavage of $FlhB_C$ (Fig. 3B). Recently, it has been shown that the *flhB*(*R320A*) mutation affecting hydrophobic interaction networks in $FlhB_{CC}$ inhibits the autocleavage of $FlhB_C$ significantly, causing a loose hook length control (35). The

flhB(*G293R*), *flhB*(*G293V*), and *flhB*(*A298V*) mutations, which reduce the rate of the autocleavage process of $FlhB_C$ considerably (16), seem to affect hydrophobic interaction networks in $FlhB_{CC}$ in a way similar to the *flhB*(*R320A*) mutation (Fig. S3B). The *flhB*(*293R*), *flhB*(*G293V*), and *flhB*(*A298V*) mutations reduced the secretion levels of filament-type proteins (Fig. 5B). Interestingly, the *flhB*(G293R) and *flhB*(A298V) mutants produced longer hooks compared to wild-type cells (Fig. 5C). Because we found that the *flhB*(*T268I*) and *flhB*(*E314A*) suppressor mutations significantly increased the probability of filament assembly in the *flhB*(*P270A*) mutant (Fig. 3), we propose that the autocleavage of $FlhB_C$ induces a conformational flexibility of $FlhB_{CN}$-$FlhB_{CC}$ boundary and that such a flexibility is important not only for the initiation of the export of filament-type proteins but also for the termination of the export of hook-type proteins at an appropriate timing of hook assembly.

How does the $FliK_C$-$FlhB_C$ interaction terminate the export of hook-type proteins? The C-terminal domain of YscP ($YscP_C$), which is a FliK homologue of the *Yersinia* injectisome, directly binds to the C-terminal domain of YscU ($YscU_C$), which is a FlhB homologue. Ala-335 of $YscU_C$, which corresponds to Ala-341 of $FlhB_C$, is critical for the binding to $YscP_C$, and Leu-280 of $YscU_C$, which corresponds to Ala-286 of $FlhB_C$, contributes to this binding (36). Ala-286, Pro-287, Ala-341, and Leu-344 form a well-conserved hydrophobic patch on the molecular surface of $FlhB_{CC}$, and this hydrophobic patch is directly involved in the recognition of the export signals of hook-type proteins (18). Therefore, we propose that the binding of $FliK_C$ to $FlhB_{CC}$ may induce a conformational change of the hydrophobic patch, thereby terminating the export of the hook-type proteins.

Flk, which is a transmembrane protein with a large cytoplasmic domain, interferes with premature switching of the substrate specificity of the flagellar type III protein export apparatus during hook-basal body assembly, and this inhibitory effect of Flk on the export of filament-type proteins is released after completion of hook assembly (9, 37–39). The *flhB*(*N269A*) and *flhB*(*P270A*) mutations interfere with the export of filament-type proteins (19), raising the possibility that these two mutations affect the negative impact of Flk on filament-type protein export. A disruption of the *flk* gene significantly increased the secretion level of FliC in the *flgE* mutant (Fig. S4), in agreement with a previous report (9). However, deletion of the *flk* gene did not increase the secretion level of FliC in the *flhB*(*N269A*) and *flhB*(*P270A*) mutants (Fig. S4), suggesting that the inability of FlhB(N269A) and FlhB(P270A) to switch export specificity does not result from failure to release the inhibitory effect of Flk on the switching. Therefore, we conclude that the autocleavage of $FlhB_C$ is critical for the flagellar type III protein export apparatus to promote the initiation of filament-type protein export.

Asp-456, Phe-459, and Thr-490 of $FlhA_C$ are involved in the interactions with the FlgN, FliS, and FliT chaperones in complex with their cognate substrates (Fig. 3B) (24–26). $FlhA_C$ adopts two distinct, open and closed conformations (40, 41), and the flagellar chaperones in complex with their cognate substrates bind to the open form of $FlhA_C$ but not to the closed form (26, 28). Interactions of $FlhA_L$ with its neighboring $FlhA_C$ subunit convert the entire $FlhA_C$ ring structure from a closed to an open form to facilitate the export of filament-type proteins (27, 28). Although it has been shown $FlhB_C$ binds to $FlhA_C$ with a micromolar affinity in solution (42), it remained unknown how $FlhB_C$ could induce a conformational change of $FlhA_C$ and promote filament-type protein export upon completion of hook assembly. Here, we found that the extragenic *flhA*(*A489E*) suppressor mutation facilitated the export of filament-type proteins even in the presence of the *flhB*(*P270A*) mutation (Fig. 3D). Interestingly, the *flhA*(*A489E*) mutation is located in the chaperone-binding site of $FlhA_C$ (Fig. 3B). Pulldown assays by GST affinity chromatography revealed that the *flhA*(*A489E*) mutation reduced the binding affinities of $FlhA_C$ for the FlgN/FlgK and FliS/FliC complexes (Fig. 4A). However, FliH and FliI overcame the defect of $FlhA_C$(A489E) in the interaction with these chaperone/substrate complexes (Fig. 4B), thereby allowing the *flhB*(*P270A*) *flhA*(*A489E*) mutant to transport FlgK and FliC at wild-type levels (Fig. 3D). Therefore, we suggest that the *flhA*(*A489E*) mutation allows $FlhA_C$ to adopt a certain conformation mimicking

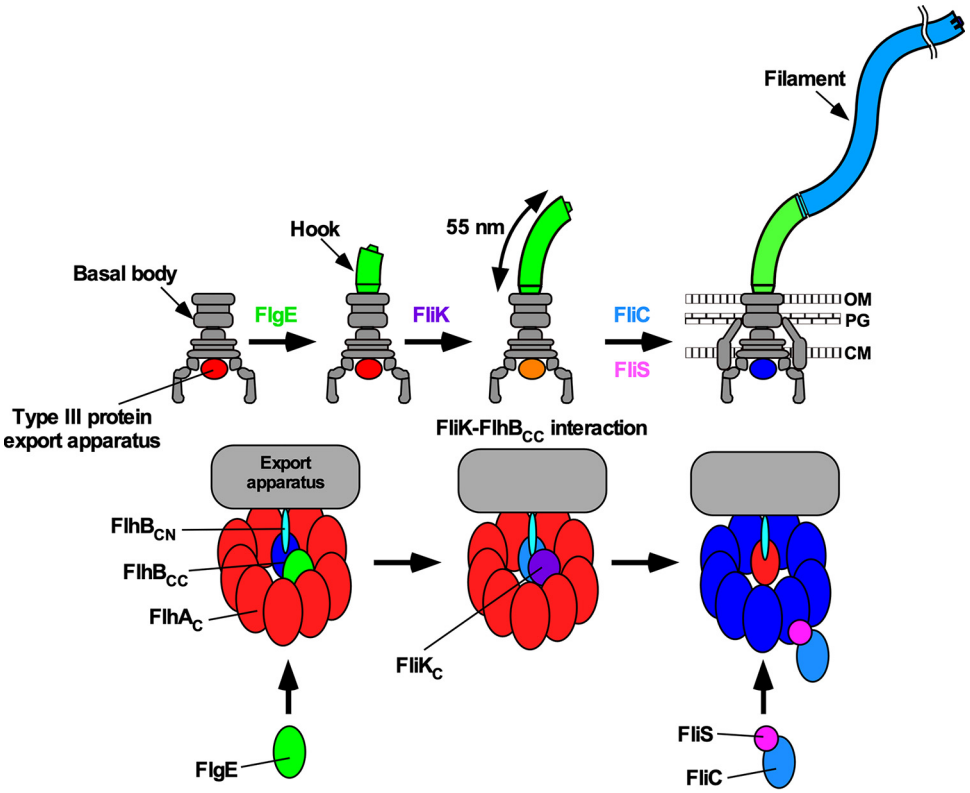

FIG 6 Model for export switching of the flagellar type III protein export apparatus. During hook assembly, the flagellar type III protein export apparatus transports the hook protein (FlgE) from the cytoplasm to the distal end of the nascent flagellar structure. The export apparatus also secretes the FliK ruler to measure the hook length during hook assembly. FlhB$_{CC}$ provides a binding site for FlgE and FliK for their efficient export. When the hook length has reached about 55 nm, the C-terminal domain of FliK (FliK$_C$) binds to FlhB$_{CC}$ to induce a conformational change of FlhB$_C$, thereby terminating the export of FlgE. Then, cleaved FlhB$_C$ binds to FlhA$_C$ to induce a structural remodeling of the FlhA$_C$ ring structure, allowing the FlgN, FliT, and FliS chaperones in complex with their cognate substrates to bind to the FlhA$_C$ ring to initiate the export of filament-type proteins to form the filament at the hook tip.

a chaperone-bound state of FlhA$_C$ even in the presence of the *flhB*(*P270A*) mutation. Introduction of the *fliK* null mutation into the *flhB*(*P270A*) *flhA*(*A489E*) suppressor mutant abolished the export of FliC but not that of FlgE (Fig. S2), suggesting that FliK is required for conformational rearrangements of the FlhA$_C$(A489E) ring structure to initiate the export of filament-type proteins. Therefore, we propose that the binding of FliK$_C$ to a cleaved form of FlhB$_C$ may promote the FlhB$_C$-FlhA$_C$ interaction to allow the FlhA$_C$ ring structure to undergo a structural transition from a closed to an open form, thereby promoting efficient docking of flagellar chaperones in complex with their cognate substrates to the FlhA$_C$ ring structure to facilitate subsequent export of filament-type proteins (Fig. 6).

MATERIALS AND METHODS

Bacterial strains, plasmids, transduction, and media. Bacterial strains and plasmids used in this study are listed in Table 1. P22-mediated transduction was carried out as described previously (43). L broth and 0.35% soft agar plates were prepared as described previously (44, 45). Ampicillin was added at a final concentration of 100 μg/ml if needed.

Site-directed mutagenesis. Site-directed mutagenesis was carried out using the QuikChange site-directed mutagenesis method (Stratagene). DNA sequencing reactions were carried out using BigDye v3.1 (Applied Biosystems); the reaction mixtures were analyzed by a 3130 Genetic Analyzer (Applied Biosystems).

Photo-cross-linking. *E. coli* BL21 Star(DE3) cells harboring pEVOL (29) and a pETDuet-based plasmid encoding both FliK(I304amber) and wild-type FlhB$_C$, FlhB$_C$(N269A), or FlhB$_C$(P270A) were exponentially grown at 30°C in L broth containing 1 mM *p*-benzoyl-phenylalanine (pBPA) and 100 μg/ml ampicillin. Then, 100 μM IPTG (isopropyl-β-D-thiogalactopyranoside) and 0.02% arabinose were added, and the incubation was continued until the culture density had reached an optical density at 600 nm (OD$_{600}$) of

TABLE 1 Strains and plasmids used in this study

Strain or plasmid	Relevant characteristics	Source or reference
Strains		
E. coli BL21 Star(DE3)	Overexpression of proteins	Novagen
Salmonella		
SJW1103	Wild type for motility and chemotaxis	43
SJW1103RflH	Δ*flk*::*tetRA*	9
MKM50	Δ*flhB*	19
MMB2701	*flhB*(*A298V*)	20
MMB2714	*flhB*(*G293R*)	20
MMB3201	*flhB*(*G293V*)	20
MM1103iK	Δ*fliK*::*tetRA*	This study
NH001	Δ*flhA*	30
NH004	Δ*fliH-fliI flhB*(*P28T*) Δ*flhA*	30
NME001	Δ*flgE*	9
NME001RflH	Δ*flgE* Δ*flk*::*tetRA*	9
TH8426	Δ*fliK*	14
TH8426RflH	Δ*fliK* Δ*flk*::*tetRA*	9
TH13763	*flhB*(*N269A*)	Kelly T. Hughes
TH13763iK	*flhB*(*N269A*) Δ*fliK*::*tetRA*	This study
TH13763RflH	*flhB*(*N269A*) Δ*flk*::*tetRA*	This study
TH12499	*flhB*(*P270A*)	Kelly T. Hughes
TH12499iK	*flhB*(*P270A*) Δ*fliK*::*tetRA*	This study
TH12499RflH	*flhB*(*P270A*) Δ*flk*::*tetRA*	This study
MMB12499-SP1	*flhB*(*P270A/T268I*)	This study
MMB12499-SP1iK	*flhB*(*P270A/T268I*) Δ*fliK*::*tetRA*	This study
MMB12499-SP2	*flhB*(*P270A/E314A*)	This study
MMB12499-SP2iK	*flhB*(*P270A/E314A*) Δ*fliK*::*tetRA*	This study
MMA12499-SP3	*flhB*(*P270A*) *flhA*(*A489E*)	This study
MMA12499-SP3iK	*flhB*(*P270A*) *flhA*(*A489E*) Δ*fliK*::*tetRA*	This study
Plasmids		
pTrc99AFF4	Modified pTrc expression vector	48
pEVOL	For incorporation of pBPA into the amber codon	29
pGEX-6p-1	Expression vector	GE Healthcare
pMKGK2	pTrc99A/FlgK	49
pMKM1002	pGEX-6p-1/GST-FliS	25
pMM104	pET19b/His-FlhA$_C$ (residues 211 to 692)	45
pMM130	pTrc99AFF4/FlhA	50
pMMGN101	pGEX-6p-1/GST-FlgN	24
pMMK521	pETDuet-1/FliK(I304amber) + FlhB$_C$	15
pMMK536	pETDuet-1/FliK(I304amber) + FlhB$_C$(N269A)	This study
pMMK537	pETDuet-1/FliK(I304amber) + FlhB$_C$(P270A)	This study
pYI101	pTrc99AFF4/FlhB	35
pYI101-SP1	pTrc99AFF4/FlhB(T268I)	This study
pYI101-SP2	pTrc99AFF4/FlhB(E314A)	This study
pYI124	pET19b/His-FlhB$_C$ (residues 211 to 383)	35
pYI140	pET19b/His-FlhB$_C$(P270A)	35
pYI140-SP1	pET19b/His-FlhB$_C$(P270A/T268I)	This study
pYI140-SP2	pET19b/His-FlhB$_C$(P270A/E314A)	This study
pYI130-SP3	pTrc99A/FlhA(A489E)	This study
pYI104-SP3	pET19b/His-FlhA$_C$(A489E)	This study

ca. 1.4 to 1.5. Photo-cross-linking experiments were performed as described previously (46). After sodium dodecyl sulfate-polyacrylamide gel electrophoresis (SDS-PAGE), immunoblotting with polyclonal anti-FliK antibody was carried out as described previously (44). Detection was done with an ECL Prime Western blotting detection reagent (GE Healthcare). Chemiluminescence signals were captured by a Luminoimage analyzer LAS-3000 (GE Healthcare). At least three independent experiments were performed.

Electron microscopy. *Salmonella* cells were grown in L broth at 30°C with shaking until the cell density had reached an OD_{600} of ca. 1.0 to 1.3. The flagella were isolated by 20 to 50% (wt/wt) sucrose density gradient ultracentrifugation as described previously (32). After ultracentrifugation at 60,000 × *g* for 60 min, the pellets were suspended in 50 mM glycine (pH 2.5) and 0.1% Triton X-100, followed by incubation at room temperature for 30 min to depolymerize flagellar filaments. After ultracentrifugation, the pellets were resuspended in 50 μl of 10 mM Tris-HCl (pH 8.0), 5 mM EDTA, and 0.1% Triton X-100. Samples were negatively stained with 2% (wt/vol) uranyl acetate. Electron micrograms were recorded with a JEM-1011 transmission electron microscope (JEOL, Tokyo, Japan) operated at 100 kV and equipped with a F415 charge-coupled device camera (TVIPS, Gauting, Germany). Hook length was measured by ImageJ, version 1.48 (National Institutes of Health).

Motility assay. Fresh colonies were inoculated onto 0.35% soft agar plates and incubated at 30°C. At least six independent measurements were carried out.

Flagellar protein export assay. Details of sample preparations have been described previously (47). Both whole-cell proteins and culture supernatants were normalized to a cell density of each culture to give a constant number of *Salmonella* cells. After heating at 95°C for 3 min, these protein samples were assessed by SDS-PAGE, followed by immunoblotting with polyclonal anti-FlgD, anti-FlgE, anti-FlgK, or anti-FliC antibody. More than five independent experiments were carried out.

Preparation of whole-cell proteins. *E. coli* BL21 Star(DE3) cells harboring a pET19b-based plasmid encoding N-terminally His-tagged $FlhB_C$ or its mutant variants were grown overnight in 5 ml of L broth containing ampicillin at 30°C with shaking. Then, 500 μl of each culture was transferred into a 1.5-ml Eppendorf tube. After centrifugation at 20,000 $\times$ *g* for 5 min, each cell pellet was suspended in 1$\times$ SDS loading buffer (the amount of loading buffer was equal to OD_{600} $\times$ 250 μl) containing 1 μl of 2-mercaptoethanol and then heated at 95°C for 3 min. Proteins in whole-cell lysates were separated by SDS-PAGE, followed by Coomassie blue staining and immunoblotting with polyclonal anti-$FlhB_C$ antibody.

Pulldown assays by GST chromatography. Detailed protocols for pulldown assays by GST affinity chromatography have been described previously (25). At least three independent experiments were carried out.

SUPPLEMENTAL MATERIAL

Supplemental material is available online only.

SUPPLEMENTAL FILE 1, PDF file, 0.7 MB.

ACKNOWLEDGMENTS

We thank Kelly T. Hughes for the kind gift of the *flhB*(*N269A*) and *flhB*(*P270A*) mutants and for critical reading of the manuscript.

This study was supported in part by the Japan Society for the Promotion of Science (JSPS KAKENHI grants JP26293097 and JP19H03182 to T.M., JP18K14638 to M.K., and JP25000013 to K.N.). This study was also partially supported by JEOL Yokogushi Research Alliance Laboratories of Osaka University to K.N.

REFERENCES

1. Nakamura S, Minamino T. 2019. Flagellum-driven motility of bacteria. Biomolecules 9:279. https://doi.org/10.3390/biom9070279.
2. Minamino T. 2014. Protein export through the bacterial flagellar type III export pathway. Biochim Biophys Acta 1843:1642–1648. https://doi.org/10.1016/j.bbamcr.2013.09.005.
3. Hirano T, Yamaguchi S, Oosawa K, Aizawa SI. 1994. Roles of FliK and FlhB in determination of flagellar hook length in *Salmonella* Typhimurium. J Bacteriol 176:5439–5449. https://doi.org/10.1128/jb.176.17.5439-5449.1994.
4. Minamino T. 2018. Hierarchical protein export mechanism of the bacterial flagellar type III protein export apparatus. FEMS Microbiol Lett 365:fny117.
5. Minamino T, Saijo-Hamano Y, Furukawa Y, González-Pedrajo B, Macnab RM, Namba K. 2004. Domain organization and function of *Salmonella* FliK, a flagellar hook-length control protein. J Mol Biol 341:491–502. https://doi.org/10.1016/j.jmb.2004.06.012.
6. Kodera N, Uchida K, Ando T, Aizawa SI. 2015. Two-ball structure of the flagellar hook-length control protein FliK as revealed by high-speed atomic force microscopy. J Mol Biol 427:406–414. https://doi.org/10.1016/j.jmb.2014.11.007.
7. Moriya N, Minamino T, Hughes KT, Macnab RM, Namba K. 2006. The type III flagellar export specificity switch is dependent on FliK ruler and a molecular clock. J Mol Biol 359:466–477. https://doi.org/10.1016/j.jmb.2006.03.025.
8. Shibata S, Takahashi N, Chevance FFV, Karlinsey JE, Hughes KT, Aizawa SI. 2007. FliK regulates flagellar hook length as an internal ruler. Mol Microbiol 64:1404–1415. https://doi.org/10.1111/j.1365-2958.2007.05750.x.
9. Minamino T, Moriya N, Hirano T, Hughes KT, Namba K. 2009. Interaction of FliK with the bacterial flagellar hook is required for efficient export specificity switching. Mol Microbiol 74:239–251. https://doi.org/10.1111/j.1365-2958.2009.06871.x.
10. Erhardt M, Hirano T, Su Y, Paul K, Wee DH, Mizuno S, Aizawa SI, Hughes KT. 2010. The role of the FliK molecular ruler in hook-length control in *Salmonella enterica*. Mol Microbiol 75:1272–1284. https://doi.org/10.1111/j.1365-2958.2010.07050.x.
11. Erhardt M, Singer HM, Wee DH, Keener JP, Hughes KT. 2011. An infrequent molecular ruler controls flagellar hook length in *Salmonella enterica*. EMBO J 30:2948–2961. https://doi.org/10.1038/emboj.2011.185.
12. Kutsukake K, Minamino T, Yokoseki T. 1994. Isolation and characterization of FliK-independent flagellation mutants from *Salmonella* Typhimurium. J Bacteriol 176:7625–7629. https://doi.org/10.1128/jb.176.24.7625-7629.1994.
13. Williams AW, Yamaguchi S, Togashi F, Aizawa SI, Kawagishi I, Macnab RM. 1996. Mutations in *fliK* and *flhB* affecting flagellar hook and filament assembly in *Salmonella* Typhimurium. J Bacteriol 178:2960–2970. https://doi.org/10.1128/jb.178.10.2960-2970.1996.
14. Minamino T, Ferris HU, Moriya N, Kihara M, Namba K. 2006. Two parts of the T3S4 domain of the hook-length control protein FliK are essential for the substrate specificity switching of the flagellar type III export apparatus. J Mol Biol 362:1148–1158. https://doi.org/10.1016/j.jmb.2006.08.004.
15. Kinoshita M, Aizawa SI, Inoue Y, Namba K, Minamino T. 2017. The role of intrinsically disordered C-terminal region of FliK in substrate specificity switching of the bacterial flagellar type III export apparatus. Mol Microbiol 105:572–588. https://doi.org/10.1111/mmi.13718.
16. Minamino T, Macnab RM. 2000. Domain structure of *Salmonella* FlhB, a flagellar export component responsible for substrate specificity switching. J Bacteriol 182:4906–4919. https://doi.org/10.1128/jb.182.17.4906-4914.2000.
17. Meshcheryakov VA, Kitao A, Matsunami H, Samatey FA. 2013. Inhibition of a type III secretion system by the deletion of a short loop in one of its membrane proteins. Acta Crystallogr D Biol Crystallogr 69:812–820. https://doi.org/10.1107/S0907444913002102.
18. Evans LD, Poulter S, Terentjev EM, Hughes C, Fraser GM. 2013. A chain mechanism for flagellum growth. Nature 504:287–290. https://doi.org/10.1038/nature12682.
19. Fraser GM, Hirano T, Ferris HU, Devgan LL, Kihara M, Macnab RM. 2003. Substrate specificity of type III flagellar protein export in *Salmonella* is controlled by subdomain interactions in FlhB. Mol Microbiol 48:1043–1057. https://doi.org/10.1046/j.1365-2958.2003.03487.x.
20. Ferris HU, Furukawa Y, Minamino T, Kroetz MB, Kihara M, Namba K, Macnab RM. 2005. FlhB regulates ordered export of flagellar compo-

nents via autocleavage mechanism. J Biol Chem 280:41236–41242. https://doi.org/10.1074/jbc.M509438200.
21. Monjarás Feria JV, Lefebre MD, Stierhof YD, Galán JE, Wagner S. 2015. Role of autocleavage in the function of a type III secretion specificity switch protein in *Salmonella enterica* serovar Typhimurium. mBio 6:e01459. https://doi.org/10.1128/mBio.01459-15.
22. Abrusci P, Vergara-Irigaray M, Johnson S, Beeby MD, Hendrixson DR, Roversi P, Friede ME, Deane JE, Jensen GJ, Tang CM, Lea SM. 2013. Architecture of the major component of the type III secretion system export apparatus. Nat Struct Mol Biol 20:99–104. https://doi.org/10.1038/nsmb.2452.
23. Bange G, Kümmerer N, Engel C, Bozkurt G, Wild K, Sinning I. 2010. FlhA provides the adaptor for coordinated delivery of late flagella building blocks to the type III secretion system. Proc Natl Acad Sci U S A 107:11295–11300. https://doi.org/10.1073/pnas.1001383107.
24. Minamino T, Kinoshita M, Hara N, Takeuchi S, Hida A, Koya S, Glenwright H, Imada K, Aldridge PD, Namba K. 2012. Interaction of a bacterial flagellar chaperone FlgN with FlhA is required for efficient export of its cognate substrates. Mol Microbiol 83:775–788. https://doi.org/10.1111/j.1365-2958.2011.07964.x.
25. Kinoshita M, Hara N, Imada K, Namba K, Minamino T. 2013. Interactions of bacterial chaperone-substrate complexes with FlhA contribute to coordinating assembly of the flagellar filament. Mol Microbiol 90:1249–1261. https://doi.org/10.1111/mmi.12430.
26. Xing Q, Shi K, Portaliou A, Rossi P, Economou A, Kalodimos CG. 2018. Structure of chaperone-substrate complexes docked onto the export gate in a type III secretion system. Nat Commun 9:1773. https://doi.org/10.1038/s41467-018-04137-4.
27. Terahara N, Inoue Y, Kodera N, Morimoto YV, Uchihashi T, Imada K, Ando T, Namba K, Minamino T. 2018. Insight into structural remodeling of the FlhA ring responsible for bacterial flagellar type III protein export. Sci Adv 4:eaao7054. https://doi.org/10.1126/sciadv.aao7054.
28. Inoue Y, Ogawa Y, Kinoshita M, Terahara N, Shimada M, Kodera N, Ando T, Namba K, Kitao A, Imada K, Minamino T. 2019. Structural insight into the substrate specificity switch mechanism of the type III protein export apparatus. Structure 27:965–976. https://doi.org/10.1016/j.str.2019.03.017.
29. Young TS, Ahmad I, Yin JA, Schultz PG. 2010. An enhanced system for unnatural amino acid mutagenesis in *Escherichia coli*. J Mol Biol 395:361–374. https://doi.org/10.1016/j.jmb.2009.10.030.
30. Hara N, Namba K, Minamino T. 2011. Genetic characterization of conserved charged residues in the bacterial flagellar type III export protein FlhA. PLoS One 6:e22417. https://doi.org/10.1371/journal.pone.0022417.
31. Minamino T, Kinoshita M, Inoue Y, Morimoto YV, Ihara K, Koya S, Hara N, Nishioka N, Kojima S, Homma M, Namba K. 2016. FliH and FliI ensure efficient energy coupling of flagellar type III protein export in *Salmonella*. MicrobiologyOpen 5:424–435. https://doi.org/10.1002/mbo3.340.
32. Inoue Y, Morimoto YV, Namba K, Minamino T. 2018. Novel insights into the mechanism of well-ordered assembly of bacterial flagellar proteins in *Salmonella*. Sci Rep 8:1787. https://doi.org/10.1038/s41598-018-20209-3.
33. Minamino T, Namba K. 2008. Distinct roles of the FliI ATPase and proton motive force in bacterial flagellar protein export. Nature 451:485–488. https://doi.org/10.1038/nature06449.
34. Zarivach R, Deng W, Vuckovic M, Felise HB, Nguyen HV, Miller SI, Finlay BB, Strynadka NC. 2008. Structural analysis of the essential self-cleaving type III secretion proteins EscU and SpaS. Nature 453:124–127. https://doi.org/10.1038/nature06832.
35. Inoue Y, Kinoshita M, Namba K, Minamino T. 2019. Mutational analysis of the C-terminal cytoplasmic domain of FlhB, a transmembrane component of the flagellar type III protein export apparatus in *Salmonella*. Genes Cells 24:408–421. https://doi.org/10.1111/gtc.12684.
36. Ho O, Rogne P, Edgren T, Wolf-Watz H, Login FH, Wolf-Watz M. 2017. Characterization of the ruler protein interaction interface on the substrate specificity switch protein in the *Yersinia* type III secretion system. J Biol Chem 292:3299–3311. https://doi.org/10.1074/jbc.M116.770255.
37. Aldridge P, Karlinsey JE, Becker E, Chevance FF, Hughes KT. 2006. Flk prevents premature secretion of the anti-sigma factor FlgM into the periplasm. Mol Microbiol 60:630–642. https://doi.org/10.1111/j.1365-2958.2006.05135.x.
38. Hirano T, Mizuno S, Aizawa SI, Hughes KT. 2009. Mutations in Flk, FlgG, FlhA, and FlhE that affect the flagellar type III secretion specificity switch in *Salmonella enterica*. J Bacteriol 181:3938–3949. https://doi.org/10.1128/JB.01811-08.
39. Kutsukake K. 1997. Hook-length control of the export-switching machinery involves a double-locked gate in *Salmonella* Typhimurium flagellar morphogenesis. J Bacteriol 179:1268–1273. https://doi.org/10.1128/jb.179.4.1268-1273.1997.
40. Moore SA, Jia Y. 2010. Structure of the cytoplasmic domain of the flagellar secretion apparatus component FlhA from *Helicobacter pylori*. J Biol Chem 285:21060–21069. https://doi.org/10.1074/jbc.M110.119412.
41. Saijo-Hamano Y, Imada K, Minamino T, Kihara M, Shimada M, Kitao A, Namba K. 2010. Structure of the cytoplasmic domain of FlhA and implication for flagellar type III protein export. Mol Microbiol 76:260–268. https://doi.org/10.1111/j.1365-2958.2010.07097.x.
42. McMurry JL, Minamino T, Furukawa Y, Francis JW, Hill SA, Helms KA, Namba K. 2015. Weak interactions between *Salmonella enterica* FlhB and other flagellar export apparatus proteins govern type III secretion dynamics. PLoS One 10:e0134884. https://doi.org/10.1371/journal.pone.0134884.
43. Yamaguchi S, Fujita H, Sugata K, Taira T, Iino T. 1984. Genetic analysis of *H2*, the structural gene for phase-2 flagellin in *Salmonella*. J Gen Microbiol 130:255–265. https://doi.org/10.1099/00221287-130-2-255.
44. Minamino T, Macnab RM. 1999. Components of the *Salmonella* flagellar export apparatus and classification of export substrates. J Bacteriol 181:1388–1394.
45. Minamino T, Macnab RM. 2000. Interactions among components of the *Salmonella* flagellar export apparatus and its substrates. Mol Microbiol 35:1052–1064. https://doi.org/10.1046/j.1365-2958.2000.01771.x.
46. Hara N, Morimoto YV, Kawamoto A, Namba K, Minamino T. 2012. Interaction of the extreme N-terminal region of FliH with FlhA is required for efficient bacterial flagellar protein export. J Bacteriol 194:5353–5360. https://doi.org/10.1128/JB.01028-12.
47. Minamino T, Kinoshita M, Namba K. 2017. Fuel of the bacterial flagellar type III protein export apparatus. Methods Mol Biol 1593:3–16. https://doi.org/10.1007/978-1-4939-6927-2_1.
48. Ohnishi K, Fan F, Schoenhals GJ, Kihara M, Macnab RM. 1997. The FliO, FliP, FliQ, and FliR proteins of *Salmonella* Typhimurium: putative components for flagellar assembly. J Bacteriol 179:6092–6099. https://doi.org/10.1128/jb.179.19.6092-6099.1997.
49. Furukawa Y, Imada K, Vonderviszt F, Matsunami H, Sano K, Kutsukake K, Namba K. 2002. Interactions between bacterial flagellar axial proteins in their monomeric state in solution. J Mol Biol 318:889–900. https://doi.org/10.1016/S0022-2836(02)00139-0.
50. Kihara M, Minamino T, Yamaguchi S, Macnab RM. 2001. Intergenic suppression between the flagellar MS ring protein FliF of *Salmonella* and FlhA, a membrane component of its export apparatus. J Bacteriol 183:1655–1662. https://doi.org/10.1128/JB.183.5.1655-1662.2001.